FINITE ELEMENT ANALYSES OF THE BEHAVIOUR OF PIPELINES WITH MULTIPLE LONGITUDINALLY ALIGNED CORROSION DEFECTS

Hélder Lima Dias Cabral, e-mail: hldcabral@yahoo.com.br
Ramiro Brito Willmersdorf, email: ramiro@willmersdorf.net
Universidade Federal de Pernambuco – Departamento de Engenharia Mecânica
Rua Acadêmico Hélio Ramos s/n – Cidade Universitária- Recife - Brasil. CEP: 50740-530

Silvana Maria Bastos Afonso da Silva, e-mail: smb@ufpe.br
Universidade Federal de Pernambuco – Departamento de Engenharia Civil
Rua Acadêmico Hélio Ramos s/n – Cidade Universitária- Recife - Brasil. CEP: 50741-500

Paulo Roberto Maciel Lyra, e-mail: prmlyra@ufpe.br
Universidade Federal de Pernambuco – Departamento de Engenharia Mecânica
Rua Acadêmico Hélio Ramos s/n – Cidade Universitária- Recife - Brasil. CEP: 50740-530

Edmundo Queiroz de Andrade, e-mail: edmundoq@petrobras.com.br
CENPES/PETROBRÁS
Cidade Universitária Quadra 7 - Ilha do Fundão – Rio de Janeiro – Brasil.

Abstract. *Corrosion is one of the most common causes of accidents involving pipelines. There are many codified semi-empirical methods available for the assessment of the integrity of corroded pipelines. However, most of these codes either do not consider the effect of interacting defects or its procedures lead to a conservative prediction of the failure pressure causing removal of pipelines prematurely. The main purpose of this work is to compute the failure pressure of pipelines with multiple corrosion defects longitudinally aligned using the finite element (FE) method and to compare the numerical results with the ones obtained via British code BS7910. Numerical analysis was performed and a parametric study was conducted varying the number of defects and the distance between them in order to investigate the effect of interaction between defects on the predicted pipeline failure pressure. The process of modeling was done using the PIPEFLAW program which has tools for generating automatically FE pipe models with corrosion defects. PIPEFLAW program, which was developed by the PADMEC research group for CENPES/PETROBRÁS during a research project, is based on the pre and pos-processor software MSC.PATRAN and it contains customized graphical interfaces for this kind of problem. Three-dimensional nonlinear analysis was performed using the solver ANSYS.*

Keywords*: corrosion defect, pipeline, finite element, Patran, graphical interface*

1. INTRODUCTION

The Finite Element Method (FEM) is one of the most efficient methodologies to quantify reliably the remaining strength of corroded pipelines. The FEM allows the direct simulation of the physical phenomena involved in the failure of the pipe, providing more precise results than the ones found through semi-empirical methods and much faster and cheaper results than the ones from experiments.

FEM analyses require, however, specific knowledge and training that are not characteristic of all pipeline engineers. The process of creating good computational models for a defect, which includes precise representation of the geometry of the defect and the generation of an appropriate mesh demands intense manual labor from the engineer, and it is also slow and extremely repetitive, therefore it is too error prone. Normally, this process is repeated from the very beginning for each new defect to be analyzed, in a clear waste of qualified human resources.

This work describes the application of PIPEFLAW program (Cabral, 2007) used to generate automatically FE pipe models with corrosion defects. This program is based on the MSC.PATRAN pre-and post-processing software (PATRAN, 2005) and has a set of computational tools which were developed with PCL (Patran Command Language) during a research project of PADMEC Research Group for CENPES/PETROBRÁS. PIPEFLAW program has a simplified and customized graphical interface, so that an engineer with basic notions of computational simulation with the FEM can generate rapidly models that result in precise and reliable simulations.

The main purpose of this work is to compute the failure pressure of pipelines with multiple corrosion defects longitudinally aligned using the finite element method and to compare the numerical results with the ones obtained via British code BS7910 (BS7910, 1999). Numerical analyses were performed and a parametric study was conducted varying the number of defects and the distance between them in order to investigate the effect of interaction between defects on the predicted failure pressure of pipes. Numerical results considering three-dimensional models generated automatically by the PIPEFLAW program were previously validated by comparing the experimental and numerical results available in literature (Cabral, 2007).

2. PIPEFLAW PROGRAM

A detailed description of the PIPEFLAW program has been published recently in a M.Sc. dissertation (Cabral, 2007). Herein, only the main steps involving the automatic generation of pipe models with corrosion defects will be presented.

PIPEFLAW program includes a set of functions and graphical interface classes implemented with PCL to generate automatically FE pipe models with corrosion defects of rectangular shape located on the internal or external pipe surface. Defects generated by the PIPEFLAW can assume the configuration of isolated defect (single defect) or multiple defects aligned (longitudinally or circumferentially). At the end of the research project, the final version of the program should include others capabilities such as defects with elliptic shape and multiple defects located at arbitrary position.

Figure 1 shows the customized graphical interface of the PIPEFLAW program integrated to the PATRAN software through a menu added on the main window which guides the user along the process of modeling. PCL Classes were specifically designed to create graphical objects (widgets) and to manage events generated by the user. Each class contains a reserved set of PCL functions which are used to define, display and update the forms and all the widgets contained in the forms.

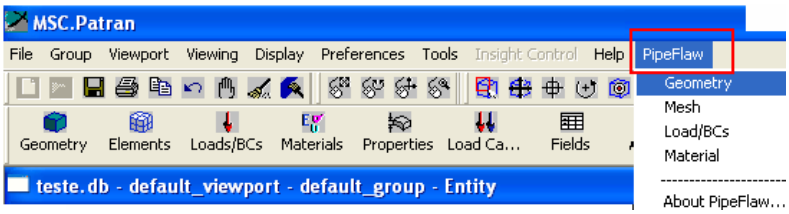

Figure 1. Main window of PATRAN with the customized PipeFlaw menu added.

The input data for the automatic generation of pipe models with corrosion defects is done entirely by graphical user interface (GUI) tools. PIPEFLAW interface has several widgets (such as window, menu, button, data box, switch, etc.) which are used by the user to interact with the program to provide the main input parameters related to the modeling process. Figure 2 shows the main window of PIPEFLAW containing various widgets where the user is able to inform the defect configuration (single or multiple defects), number of defects, pipe dimensions (diameter, thickness and length), defect shape (rectangular or elliptic) and the defect location (internal or external pipe surface). If the user "clicks" on the "Defect Parameters" button, a new window appears inviting the user to provide the defect dimensions (depth "D", circumferential length "LC", longitudinal length "LL" and the fillet radius "RA" and "RC") as indicated in the right window of Fig. 2.

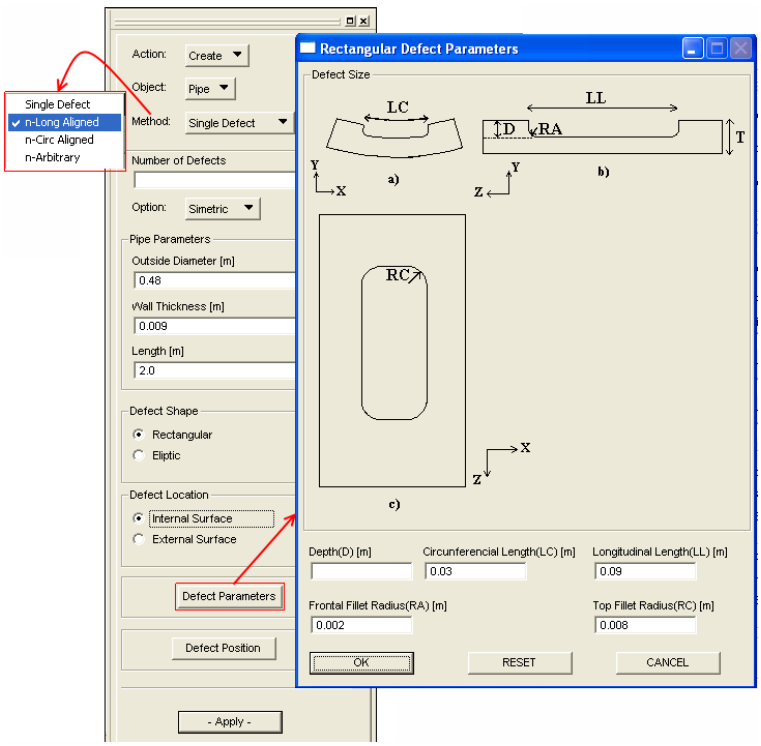

Figure 2. Main window of PIPEFLAW (left) and window for input data of rectangular defect dimensions (right).

If the user "clicks" on the "Defect Position" button, another window appears and the user has to provide through data boxes the positions of each defect along the pipe. For the multiple longitudinally aligned defect case, the user has to enter the distance (in meters) of the centre of each defect. Similarly, for the case of multiple defects aligned in circumferential direction, the user should enter the angular position (in degrees) of the centre of each defect. For both cases, the respective window has customized icons illustrating how the user should enter the parameters.

2.1. Automatic Mesh Generation

The automatic process of modeling is executed by several implemented PCL functions that, together with the graphical user interface classes, compose the PIPEFLAW program. After the user have been entered all modeling parameters via graphical interface, the automatic generation of the model is initiated. The first step performed by the PIPEFLAW is the automatic generation of the geometry and mesh of the defect region (see Fig. 3). The program computes the element thickness inside the defect region by dividing the remaining wall thickness (T-D) by four (defects generated by the PIPEFLAW has always four elements along the wall thickness in the defect region). The element thickness is used as a parameter to compute automatically the number of elements along all edges of the solids on the model. This produces an aspect ratio around unit in elements inside defect region. The solid FE models can be generated by PIPEFLAW using linear Hex8 elements or quadratic Hex20 elements available in MSC.PATRAN Library. The models presented here were constructed using linear Hex8 elements.

The second step of the automatic modeling procedure is the generation of six adjacent regions of the defect which are used to reduce the model size. As shown in Fig. 3, the modeling of adjacent regions includes: one region for mesh transition along the pipe thickness (from four elements reduces to two elements), three regions for mesh transition along the surface and two expansion regions (no mesh transition). This mesh density was selected based on a convergence study executed by the PETROBRÁS R&D Center in which nonlinear analyses were performed using an increasing degree of mesh refinement.

The third and last step is the generation of pipe model with single or multiple defects. For the single defect case, complementary solids and meshes of one quarter of the pipe are generated taking advantage of symmetry conditions. Multiple defects are generated through translations (multiple defects longitudinally aligned) and rotations (multiple defects circumferentially aligned) of previously created defect and adjacent regions. To connect one defect to another, new geometry and mesh are created between adjacent defects.

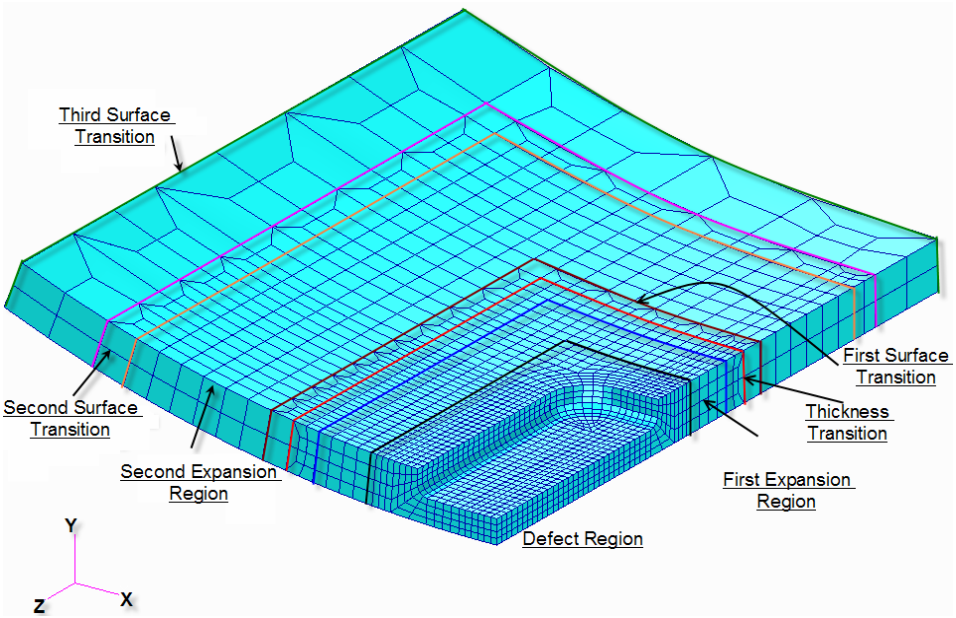

Figure 3. Default mesh discretization generated by the PIPEFLAW including the defect region and six adjacent regions.

3. VALIDATION

This section presents results from FE simulation executed by Cabral (2007) to validate the PIPEFLAW program. The validation consisted of simulating three of six specimens which were previously investigated experimentally by Benjamin et al (2005) and numerically by Andrade et al (2006). Figure 4 shows the configuration of the rectangular machined defects contained in the three specimens modeled using the PIPEFLAW program: IDTS2 (single defect), IDTS3 (two defects longitudinally aligned) and IDTS4 (two defects circumferentially aligned). The rectangular defects are located at the external surface of the pipe and the main dimensions are presented in Tab. 1.

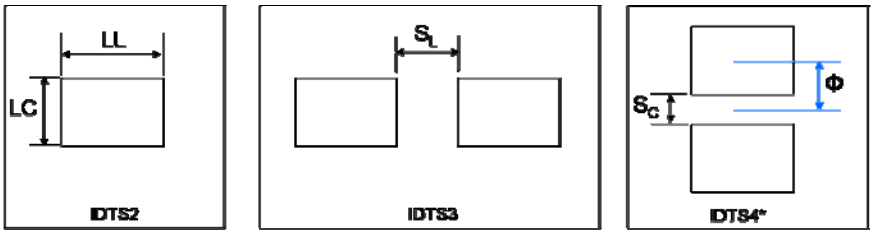

Figure 4. Defect configurations of the specimens investigated by Benjamin et al (2005) and Andrade et al (2006).

Table 1. Actual dimensions of the tubular specimens and of the machined defects. Source: Andrade et al (2006)

Specimen	LL [mm]	LC [mm]	D [mm]	RA [mm]	RC** [mm]	S_L [mm]	S_C [mm]	S_C^* [mm]	$\frac{D}{T}\cdot 100[\%]$
IDTS2	39.6	31.9	5.39	3.5	8.0	-	-	-	66.5%
IDTS3	39.6	31.9	5.32	3.5	8.0	20.5	-	-	65.7%
IDTS4*	39.6	32.0	5.62	3.5	8.0	-	9.9	11.65	69.4%
DE = 458.8 mm (pipe outside diameter)									
T = 8.1 mm (pipe wall thickness)									

Note: * → Minimum spacing used by the PIPEFLAW.
** → Actual value unknown. S_L e S_C = Longitudinal and Circunferencial spacing, respectively.

PIPEFLAW program uses an angle Φ (in degrees) as a distance parameter between defects circumferentially aligned. The angle Φ equivalent to the actual distance of 9.9mm (specimen IDTS4) is 5.23º. However, the angle used for the specimen IDTS4 was 5.45º (equivalent to a distance of SC^* = 11.65mm). Therefore, due to this small difference, the model IDTS4 used in the validation was named as IDTS4*.

Appropriate boundary conditions were applied at the symmetry planes when applicable. Pressure was incrementally applied to the internal surfaces of the model and longitudinal force due to the internal pressure was simultaneously applied to the pipe wall at the cut-off boundary of the models. The ANSYS program (ANSYS, 2004) was employed to perform the finite element analyses which accounted for geometrical and physical nonlinearities.

The material properties used in the FE simulations, which were the same used by Andrade et al (2006), assume a rate-independent plasticity model using the von Mises yield criterion and adopts an isotropic hardening rule. The values of Young modulus, yield stress and true ultimate tensile stress are, respectively: 200,000.0MPa, 534.1MPa and 718.2MPa. The true stress-true strain curve of material was constructed based on the Ramberg-Osgood equation of the material (Eq. 1) determined experimentally by Benjamin et al (2005).

$$\varepsilon^* = \frac{\sigma^*}{E} + 0.0788174 \cdot \left(\frac{\sigma^*}{\sigma^*_u} \right)^{12.642026} \tag{1}$$

where ε^*, σ^* and σ^*_u are the true strain, true stress and the true ultimate tensile stress, respectively.

Table 2 presents the failure pressures measured in the laboratory tests by Benjamin et al (2005), the failure pressures predicted by FE simulations conducted by Andrade et al (Pf_1) and Cabral (Pf_2) and the failure pressures predicted through semi-empirical method (BS-7910). The failure criterion adopted by Cabral was the same used by Andrade et al and establishes that failure is reached when the von Mises stress along a radial direction (all points situated across the thickness), within the colony of defects, exceeds the true ultimate tensile stress (σ^*_u). The errors of the predicted failure pressures are also presented in Tab. 2.

Table 2. Actual and predicted failure pressures.

	Failure Pressures [MPa]				Error[1] (%)		
	Experimental	FE Simulations		BS7910	FE Simulations		BS7910
Specimen	$Pf_{(EXP)}$	Pf_1	Pf_2	Pf_3	E_1	E_2	E_3
IDTS2	22.679	22.710	22.791	21.253	+0.14	+0.49	-6.29
IDTS3	20.314	19.535	19.810	18.511	-3.83	-2.48	-8.88
IDTS4	21.138	22.298	22.403*	20.944	+5.49	+5.98*	-0.92
mean[2]	-	-	-	-	3.15	2.98	5.36

Note: * – Values associated with the model IDTS4* used by Cabral (2007).
1 – Error (%) = [(Pf_i - Pf_{EXP}) / (Pf_{EXP})] . 100% (i = 1, 2 e 3) 2 – Mean = ∑ | Error | /3

It should be noted that the errors obtained by FE simulations were quite similar and showed excellent agreement with the experimental results. Failure pressures were within -3.83% and +5.49% for Andrade et al (2006) and within -2.31% and +5.98% for Cabral (2007). The failure pressures predicted by the BS7910 method presented more conservative values comparing with the ones obtained by FE simulations and were within -8.88% and -0.92% which confirms the conservative assessment embodied in this semi-empirical method. However, for these cases, BS7910 results showed also good agreement with the experimental results.

3. PARAMETRIC STUDY

The use of PIPEFLAW program for generating automatically FE pipe models with corrosion defects has prove to be an excellent tool to create rapidly reliable FE models. With the use of PIPEFLAW tools one can accelerate the process of modeling and make easy the execution of parametric studies. In the present work, it will be investigated the behavior of pipelines subjected to multiple defects aligned in the longitudinal direction. The main objective of this study is to evaluate the effect of interaction between defects in the failure pressure of corroded pipes.

The methodology of the parametric study was done varying the distance between defects and the number of interacting defects. Three groups of pipe models were analyzed containing two, three and four identical defects aligned in the longitudinal direction of the pipe. In order to investigate the effect of interaction between defects, for each group of pipe models it was generated a series of seven models with defects equally spaced with a total of 21 FE models. For the first model of each group, a distance SL (see Fig. 4) equivalent to two pipe wall thickness (2T) was used. For the other six models of each group, it was used a distance SL equivalent to three (3T), four (4T), five (5T), six (6T), ten (10T) and fifteen (15T) pipe wall thicknesses, respectively.

Table 3 presents the pipe dimensions (outside diameter - DE, wall thickness – T, length - LD) and the dimensions of the investigated defects. The FE models are identified by a name indicating the configuration of defects (MD – multiple defects or SD – single defect), the number of defects longitudinally aligned (2L, 3L or 4L) and the spacing distance between defects (2T, 3T, 4T, 5T, 6T, 10T or 15T). Numerical simulations considering isolated (or single) defects were also executed in order to compare with the results of multiple defect cases. Four FE models with single defects were analyzed (SD_LL1, SD_LL2, SD_LL3 and SD_LL4) as shown in Tab. 3. The defect dimensions are the same, except the longitudinal length (LL) which varied. The model SD_LL1 represents the isolated defect with longitudinal length equal to 40.0 mm (the same value used for the multiple defect models). The other three FE models with single defects (SD_LL2, SD_LL3 and SD_LL4) were analyzed to investigate the effect of longitudinal defect length in the failure pressure of pipes. These three single defect FE models represent the limit situation where the multiple defects of each group are touching (spacing S_L between defects is null). For these situations, the touching defects are expected to behave as a unique composed longer defect with longitudinal length equal to two, three and four times the longitudinal length of the single defect of model SD_LL1.

Table 3. Dimensions of the FE pipe models with rectangular defects.

Pipe dimensions			Rectangular defect dimensions					
DE[mm]	T[mm]	LD[mm]	LL[mm]	LC[mm]	D[mm]	RA[mm]	RC[mm]	(D/T).100%
480.0	9.0	2500.0	40.0	30.0	5.4	2.0	8.0	60%

Multiple defects							
Models	MD_2L_2T	MD_2L_3T	MD_2L_4T	MD_2L_5T	MD_2L_6T	MD_2L_10T	MD_2L_15T
	MD_3L_2T	MD_3L_3T	MD_3L_4T	MD_3L_5T	MD_3L_6T	MD_3L_10T	MD_3L_15T
	MD_4L_2T	MD_4L_3T	MD_4L_4T	MD_4L_5T	MD_4L_6T	MD_4L_10T	MD_4L_15T
Distance S_L [mm]	18.0	27.0	36.0	45.0	54.0	90.0	135.0

Single Defects				
Models	SD_LL1	SD_LL2	SD_LL3	SD_LL4
LL[mm]	40.0	80.0	120.0	160.0

Table 4 presents the results of predicted failure pressure of the FE models which were analyzed using the same material, boundary conditions and failure criterion of the validation models described previously. The correspondent failure pressures predicted through semi-empirical method BS7910 are also presented. All predicted failure pressures using BS7910 method presented more conservative results when compared with the FE predictions, especially for longer defects. The failure pressure predicted via BS7910 method for the model SD_LL4 (with the longest single defect) was -12.15% less than the one predicted via the FEM while for the model SD_LL1 (the shorter single defect) the semi-empirical value differed -4.74% from the FEM result.

Figure 5 shows the predicted FE failure pressures plotted in as a function of the distance between defects for the three groups analyzed with two (MD_2L), three (MD_3L) and four (MD_4L) defects. The correspondent values for the single defect cases are also indicated by four different lines. As indicated in Fig. 5, the failure pressures appear to be more influenced by the number of defects rather than their separation especially for the cases where the defects are

separated by a small distance. However, this influence does not appear to continue indefinitely as indicated in the graph where the gap between curves MD-2L and MD-3L is greater than the gap between curves MD-3L and MD-4L. As expected, increasing the distance between defects, the predicted failure pressures tend to reach the superior value of 24.583MPa equivalent to the failure pressure of the single defect case (SD_LL1) with an asymptotic behavior.

Table 4. Failure pressure predicted via FEM and BS7910 method.

Single defects							
Model	SD_LL1		SD_LL2		SD_LL3	SD_LL4	
Pf_{FEM}[MPa]	24.583		22.182		19.790	17.876	
Pf_{BS}[MPa]	23.418		20.088		17.455	15.705	
Group of 2 defects (MD-2L)							
Model	MD_2L_2T	MD_2L_3T	MD_2L_4T	MD_2L_5T	MD_2L_6T	MD_2L_10T	MD_2L_15T
Pf_{FEM}[MPa]	22.315	22.782	23.07	23.24	23.42	23.915	24.315
Pf_{BS}[MPa]	20.695	20.876	21.021	21.145	21.255	21.621	23.418
Group of 3 defects (MD-3L)							
Model	MD_3L_2T	MD_3L_3T	MD_3L_4T	MD_3L_5T	MD_3L_6T	MD_3L_10T	MD_3L_15T
Pf_{FEM}[MPa]	20.640	21.315	21.731	22.115	22.470	23.440	24.070
Pf_{BS}[MPa]	18.864	19.301	19.658	19.964	20.232	21.061	23.418
Group of 4 defects (MD-4L)							
Model	MD_4L_2T	MD_4L_3T	MD_4L_4T	MD_4L_5T	MD_4L_6T	MD_4L_10T	MD_4L_15T
Pf_{FEM}[MPa]	19.315	20.261	21.070	21.600	22.070	23.315	24.040
Pf_{BS}[MPa]	17.793	18.438	18.959	19.395	19.769	20.866	23.418

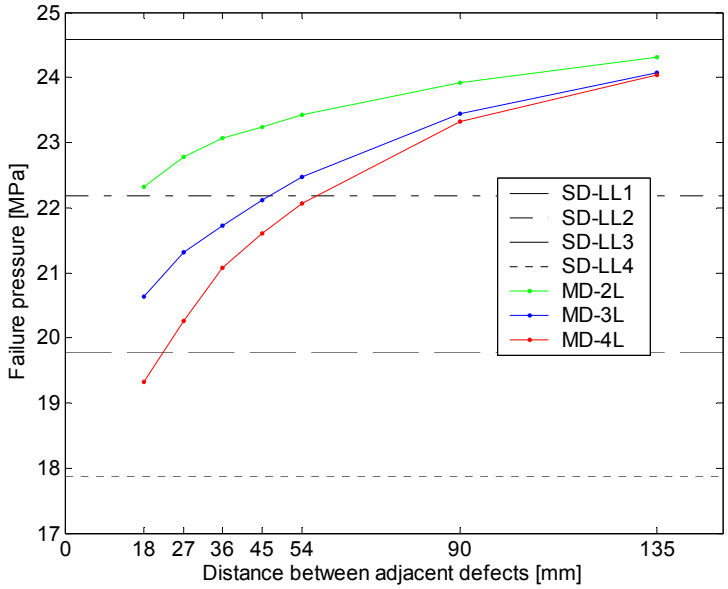

Figure 5. Predicted FE failure pressure *vs.* distance between defects.

Figures 6 to 9 present the contour plots of von Mises equivalent stress together with the deformed configuration of the corroded region for the FE models with single defect (these plots were drawn applying a scale factor of 5 to the displacements). In all single defect FE models, the highest von Mises stress occurs near the region of the frontal fillet radius of the defect along the longitudinal direction of the pipe, as indicated in the plots by the longitudinal red strips.

Figure 10 presents the results of von Mises stress variations against pressure values for the four single defect models. These results were obtained at a point located at the most stressed region on the internal pipe surface. As suggested in the BS7910, appendix G, stress variations with increased pressure load (for all models) showed three distinct stages. The first is a linear response progressing to a point when the elastic limit is reached (σ_y = 534.1MPa). On the second stage, the maximum von Mises stress remains approximately constant or increase slowly (plasticity spreads through the remaining ligament). The third stage is dominated by material hardening progressing to the point where failure occurs.

Results of displacements variations (in y direction) against pressure values provided by the non-linear FE analysis for the four single defect models are presented in Fig. 11. All four curves were plotted for a point located at the center of the corroded area on the internal pipe surface. Comparing Fig. 11 with Fig. 10, one can observe a linear response of

the displacements progressing to the point where the third stage of Fig. 10 is initiated. After this point, the results of displacements increase rapidly with the increased pressure presenting an asymptotic behavior.

In previous studies (Chouchaoui and Pick, 1994; Cabral et al, 2007) it was shown that circumferentially aligned corrosion defects do not interact, even when defects are touching. In contrast with this, it was shown that for longitudinally aligned corrosion defects (Chouchaoui and Pick, 1996) by decreasing the distance between them they begin to interact reducing the remaining strength of the corroded pipe. Here this is confirmed in figures 12, 14 and 16 which present the contour plots of the von Mises stress for the models with defects separated by the smallest distance of 2T. For this situation, defects interacted as indicated by the two highest stress levels (red and yellow strips) located at the central defect. These figures show a high stress level in the remaining ligament of the central defects, which confirms the tendency of the central defect in a group of longitudinally aligned defects to fail first. In addition, the highest stress level (red strips) occurs through the full thickness pipe material between the central defects suggesting that in a limit situation, where adjacent defects are touching, defects will behave as single longer defect (compare figures 7, 8 and 9 with figures 12, 14 and 16).

The BS7910 interaction rules applied to the models with two, three and four defects separated by 15T treat the defects as isolated due to the fact that the axial spacing of 15T exceeds the value of $2 \cdot \sqrt{DE.T}$. This rule appears to be a good consideration as indicated by the contour plots of von Mises stress for the correspondent models in figures 13, 15 and 17, respectively. These stress contours are almost identical to those of the isolated defect (Fig. 6) suggesting that no effective interaction occurred. This can also be confirmed in Fig. 18 which presents the von Mises stress variations against pressure values for five models of the group containing four defects aligned. The curves for the models MD_4L-15T is almost overlaying the curve equivalent to the isolated defect model (SD_LL1). Figure 19 shows the von Mises stress variations against pressure values for the models with two, three and four defects separated by the same distance of 2T. As expected, the three curves lay between the curves of the isolated defect models SD_LL1 and SD_LL4. Increasing the number of defects, the curves begin to incline towards left near the region of material hardening stage progressing to the failure point.

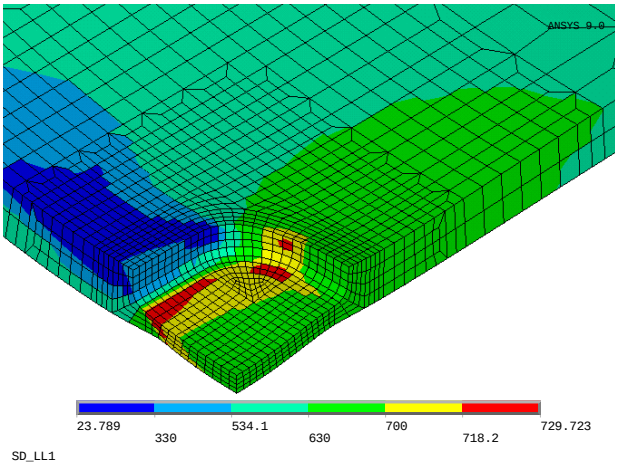

Figure 6. von Mises stresses for the model SD_LL1.

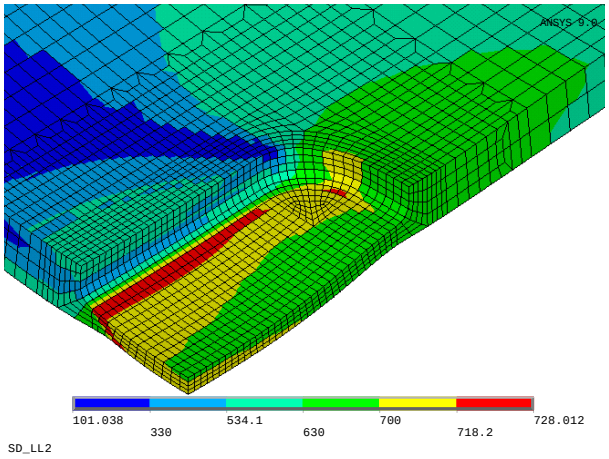

Figure 7. von Mises stresses for the model SD_LL2.

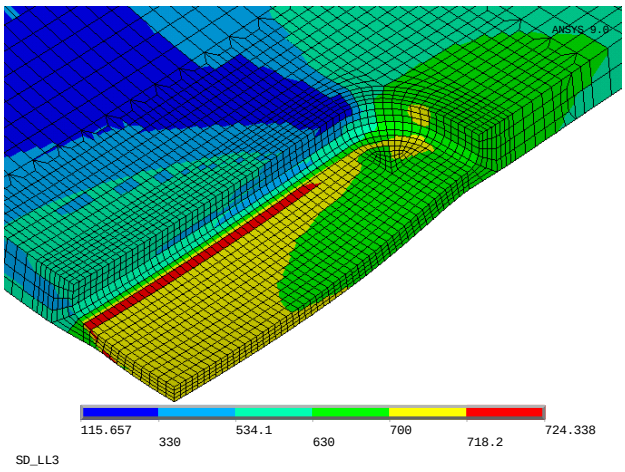

Figure 8. von Mises stresses for the model SD_LL3.

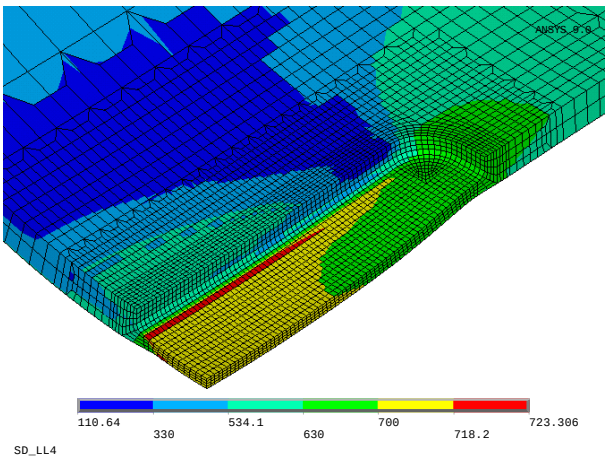

Figure 9. von Mises stresses for the model SD_LL4.

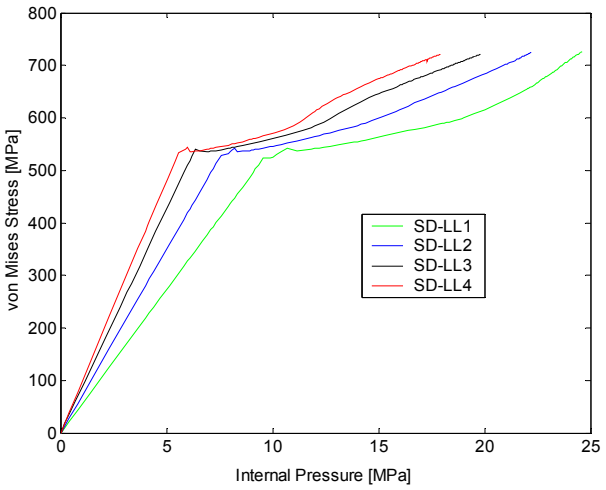

Figure 10. von Mises stress variations against pressure values for the single defect models.

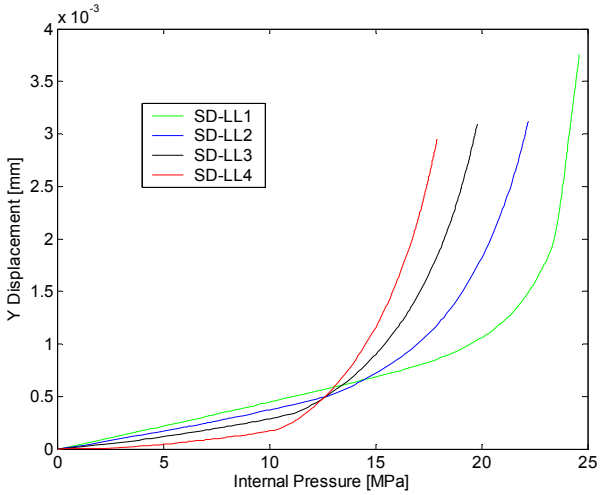

Figure 11. Displacement variations against pressure values for the single defect models.

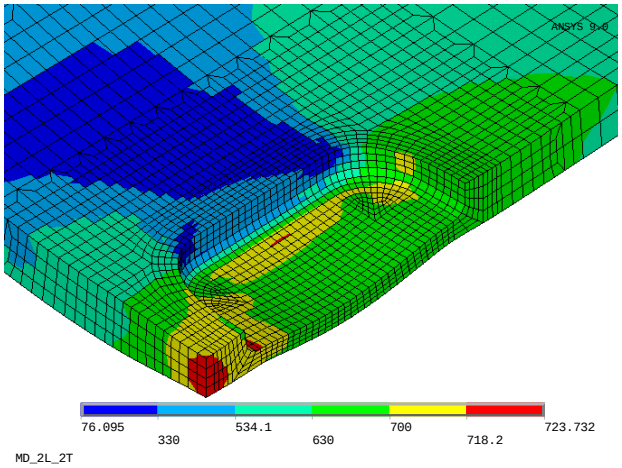

Figure 12. von Mises stresses for the model MD_2L_2T.

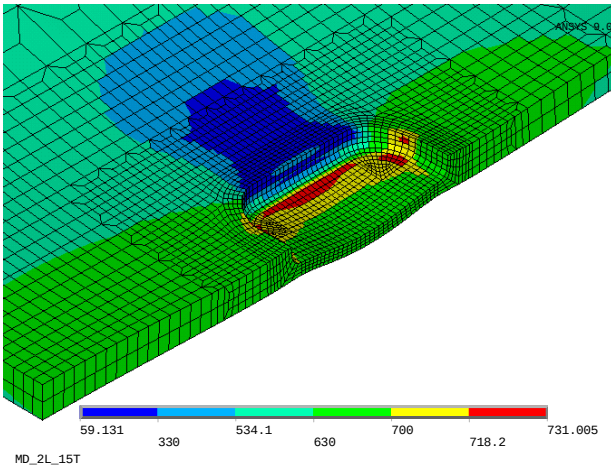

Figure 13. von Mises stresses for the model MD_2L_15T.

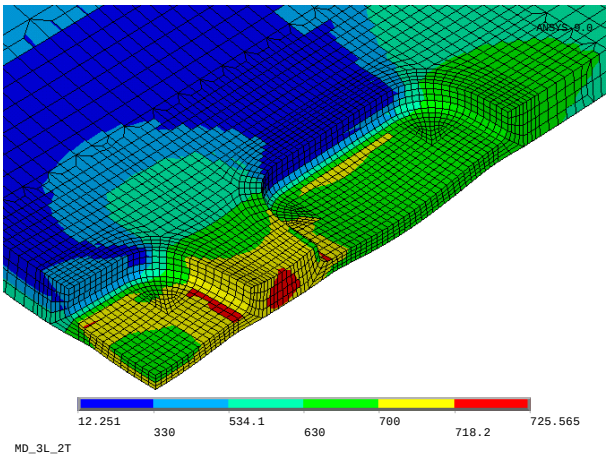

Figure 14. von Mises stresses for the model MD_3L_2T.

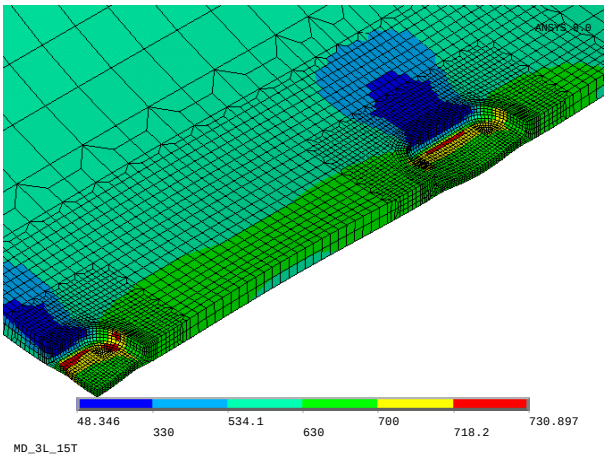

Figure 15. von Mises stresses for the model MD_3L_15T.

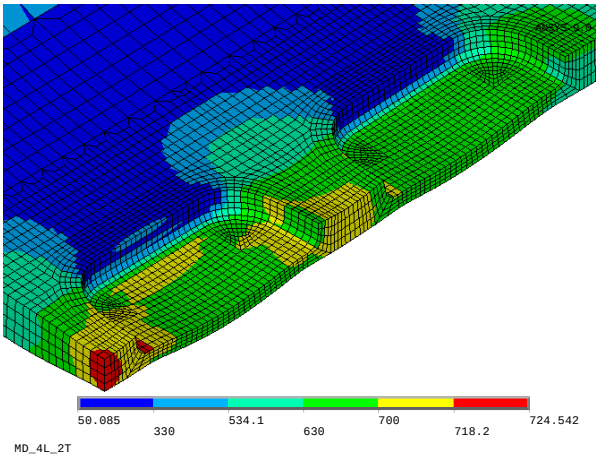

Figure 16. von Mises stresses for the model MD_4L_2T.

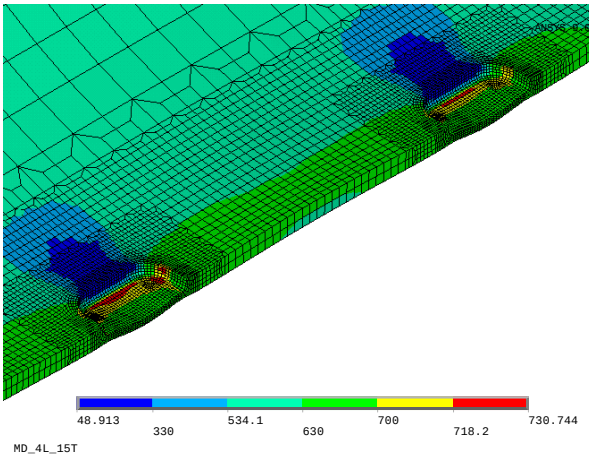

Figure 17. von Mises stresses for the model MD_4L_15T.

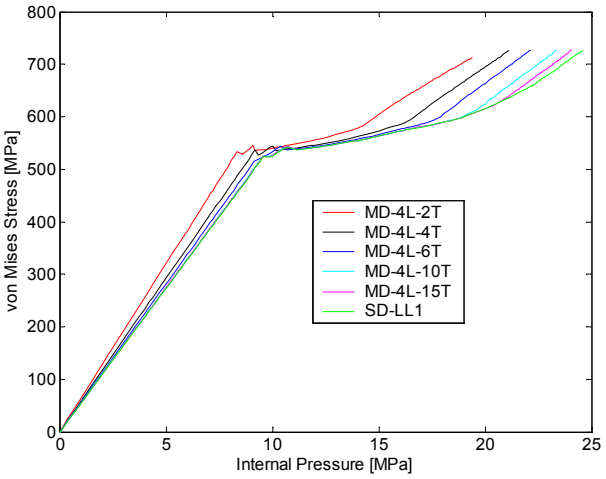

Figure 18. von Mises stress variations against pressure values for MD_4L models: influence of distance between defects.

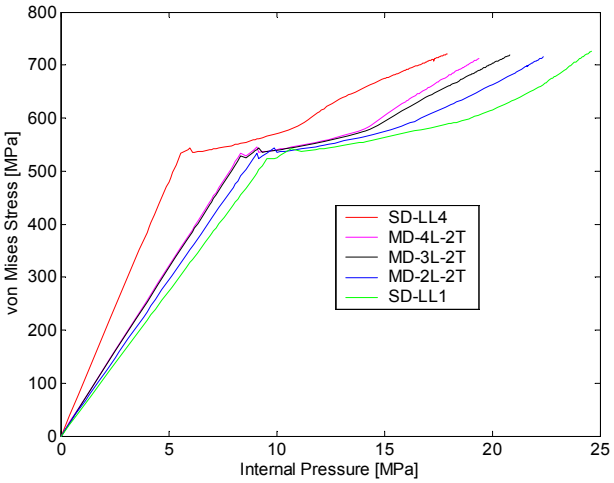

Figure 19. von Mises stress variations against pressure values for models with defects separated by 2T: influence of the number of defects.

4. CONCLUSIONS

The PIPEFLAW tools for generating automatically FE pipe models with corrosion defects were applied successfully in this work. These tools showed a rapid way of generating reliable FE models facilitating the parametric study presented here.

The graphical user interface tools provided by the PIPEFLAW program enables the user to enter the input modeling parameters in an intuitive and friendly way so that an engineer with basic notions of computational simulation with the FEM can generate rapidly models that result in precise and reliable simulations.

Results obtained by the parametric study confirmed that multiple defects aligned in the longitudinal direction interact reducing the remaining strength of the corroded pipe. In addition, in a group of defects longitudinally aligned, the central defect will have the tendency to fail first.

5. ACKNOWLEDGEMENTS

The authors would like to thank PETROBRÁS for permission to publish this paper, for supplying the experimental and numerical data used in the validation portion of this study and for giving supporting guidance throughout the course of this research project. The authors also wish to thank FINEP-Brazil, CAPES and CNPq for the financial support of various research projects developed in this area by the PADMEC Research Group.

6. REFERENCES

Andrade, E.Q., Benjamin, A.C., Machado Jr., P.R.S., Pereira, L.C., Jacob, B.P., Carneiro, E.G., Guerreiro, J.N.C., Silva, R.C.C., Noronha Jr., D.B., 2006. "Finite Element Modeling of the Behavior of Pipelines Containing Interacting Corrosion Defects". 25th International Conference on Offshore Mechanics and Arctic Engineering (OMAE2006-92600), Hamburg, Germany.

ANSYS, 2004. "Ansys Release 9.0 Documentation: Operations Guide(Chapter 3) and Structural Guide (Chapter 8)". http://www.ansys.com.

Benjamin, A.C., Freire, J.L.F., Vieira, R.D., Diniz, J.L.C., Andrade, E.Q., 2005. "Burst Tests on Pipeline Containing Interacting Corrosion Defects". Proc. 24th International Conference on Offshore Mechanics and Arctic Engineering (OMAE2005), Halkidiki, Greece.

BS7910, 1999. "Guide on Methods for Assessing the Acceptability of Flaws in Metallic Structures – Annex G: The Assessment of Corrosion in Pipes and Pressure Vessels", British Standard.

Cabral, H.L.D., 2007. "Desenvolvimento de Ferramentas Computacionais para Modelagem e Análise Automática de Defeitos de Corrosão em Dutos". Programa de Pós-Graduação em Engenharia Mecânica, UFPE, Recife, Dissertação de Mestrado, 140p.

Cabral, H.L.D., Willmersdorf, R.B., Afonso, S.M.B., Lyra, P.R.M., Andrade, E.Q., 2007. "Modelagem e Análise Automática de Dutos com Múltiplos Defeitos de Corrosão Alinhados Circunferencialmente", CMNE/CILAMCE2007, ID 1108 (accepted for publication), Porto, Portugal.

Chouchaoui, B.A. and Pick, R.J., 1994. "Behaviour of Circumferentially Aligned Corrosion Pits", International Journal of Pressure Vessels and Piping, v.57, pp.187-200.

Chouchaoui, B.A. and Pick, R.J., 1996. "Behaviour of Longitudinally Aligned Corrosion Pits", International Journal of Pressure Vessels and Piping, v.67, pp.17-35.

PATRAN, 2005. "Help system: MSC.Patran Library (PCL Manuals) and MSC.Acumen Library (Develop Manuals)". http://www.mscsoftware.com.

5. RESPONSIBILITY NOTICE

The authors are the only responsible for the printed material included in this paper.